A Viscoelastic Higher-Order Beam Finite Element

A. R. Johnson[†] and A. Tessler
Computational Structures Branch
NASA Langley Research Center, MS 240
Hampton, VA 23681-0001

ABSTRACT

A viscoelastic internal variable constitutive theory is applied to a higher-order elastic beam theory and finite element formulation. The behavior of the viscous material in the beam is approximately modeled as a Maxwell solid. The finite element formulation requires additional sets of nodal variables for each relaxation time constant needed by the Maxwell solid. Recent developments in modeling viscoelastic material behavior with strain variables that are conjugate to the elastic strain measures are combined with advances in modeling through-the-thickness stresses and strains in thick beams. The result is a viscous thick-beam finite element that possesses superior characteristics for transient analysis since its nodal viscous forces are not linearly dependent on the nodal velocities, which is the case when damping matrices are used. Instead, the nodal viscous forces are directly dependent on the material's relaxation spectrum and the history of the nodal variables through a differential form of the constitutive law for a Maxwell solid. The thick beam quasistatic analysis is explored herein as a first step towards developing more complex viscoelastic models for thick plates and shells, and for dynamic analyses.

The internal variable constitutive theory is derived directly from the Boltzmann superposition theorem. The mechanical strains and the conjugate internal strains are shown to be related through a system of first-order, ordinary differential equations. The total time-dependent stress is the superposition of its elastic and viscous components. Equations of motion for the solid are derived from the virtual work principle using the total time-dependent stress. Numerical examples for the problems of relaxation, creep, and cyclic creep are carried out for a beam made from an orthotropic Maxwell solid.

INTRODUCTION

Advanced composites technology has led to the use of highly viscous, low-modulus materials that are combined with the traditional high-modulus, load carrying materials to produce stiff, highly damped structures. The quasi-static and dynamic analyses of such

---

[†] Vehicle Structures Directorate, Army Research Laboratory.

structures require improvements in the material damping representation over the standard proportional damping schemes. Halpin and Pagano[1] demonstrated that the relaxation moduli for anisotropic solids produce symmetric matrices that can be expanded in a Prony series form (i.e., a series of exponentially decaying terms). Early viscoelastic models for small deformations of composites focused on computing the complex moduli for anisotropic solids from the elastic properties of the fibers and the complex modulus properties of the matrix[2,3]. Recently, various classical constitutive models have been used including generalized Maxwell and Kelvin-Voigt solids[4,5]. These constitutive models have practical value since they provide adequate approximations for the dynamic softening and hysteresis effects – the phenomena that are not directly proportional to strain rates.

In this paper, a brief review of the history integral form of the Maxwell solid is presented to provide background for the differential constitutive law. The interested reader is referred to Coleman and Noll[6] and Schapery[7] for more comprehensive discussions on the subject. A new differential constitutive law for the Maxwell solid is then derived. This form is a special case of the model developed by Johnson and Stacer[8] for large strain viscoelastic deformations of rubber. It has also been used by Johnson et al.[9,10] to formulate a viscoelastic, large-displacement shell finite element. The differential constitutive law is then combined with the higher-order beam theory and finite element formulation of Tessler[11] providing viscoelastic capability for thick beams. The additional strain variables required in the constitutive law are replaced with element nodal variables that are conjugate to the elastic nodal variables. This results in only minor modifications to the elastic finite element code. Finally, several numerical examples are presented demonstrating the viscoelastic, thick-beam response under quasi-static loading.

MAXWELL SOLID IN HISTORY INTEGRAL FORM

The stress-strain relation for a linear elastic material can be written in the tensor form as

$$\sigma_{ij} = C_{ijkl}\varepsilon_{kl} \tag{1}$$

where σ_{ij} are the stress components, C_{ijkl} are the elastic stiffness coefficients, and ε_{kl} are the strains. When a linear viscoelastic material is subjected to an instantaneous incremental strain, $\Delta\varepsilon_{kl}$, the time dependent stress takes the form

$$\sigma_{ij}(t) = C_{ijkl}\Delta\varepsilon_{kl} + \sigma_{ij}^{v}(t) \tag{2}$$

where the viscous stresses, $\sigma_{ij}^{v}(t)$, are monotonically decreasing functions of time. The Boltzmann superposition method is often used to approximate Eq(2) as follows. The viscous stresses, $\sigma_{ij}^{v}(t)$, are factored such that

$$\sigma_{ij}^{v}(t) = C_{ijkl}^{v}(t)\Delta\varepsilon_{kl} \tag{3}$$

The functions $C_{ijkl}^{v}(t)$ are referred to as time dependent moduli. These monotonically decreasing functions are approximated in time using a Prony series, i.e.,

$$C_{ijkl}^{v}(t) = C_{ijkl}^{*}\sum_{n=1}^{N} e^{-\frac{t}{\tau_n}} \tag{4}$$

where $\tau_n, C_{ijkl}^{*} \geq 0$. The stresses then become

$$\sigma_{ij}(t) = C_{ijkl}\Delta\varepsilon_{kl} + \sum_{n=1}^{N} C_{ijkl}^{*} e^{-\frac{t}{\tau_n}}\Delta\varepsilon_{kl} \tag{5}$$

The above approximation is extended to the case of a continuously deforming solid by associating the continuous time dependent strain with an incremental strain history and convoluting Eq(5) in time. The approximation to the time dependent stresses becomes

$$\sigma_{ij}(t) = C_{ijkl}\sum_{m=1}^{M}\Delta_m\varepsilon_{kl} + \sum_{n=1}^{N} C_{ijkl}^{*}\sum_{m=1}^{M} H(t-t_m)e^{-\frac{(t-t_m)}{\tau_n}}\Delta_m\varepsilon_{kl} \tag{6}$$

where the strain increments are set at times t_m for $m = 1,...,M$, and use is made of the Heaviside unit step function, $H(t-t_m)$. At this juncture, it is often customary to define the viscous moduli as functions of the relative time, $t-t_m$, i.e.,

$${}^{*}C_{ijkl}(t-t_m) = \sum_{n=1}^{N} C_{ijkl}^{*} H(t-t_m)e^{-\frac{(t-t_m)}{\tau_n}} \tag{7}$$

The constitutive model in Eq(6) then takes the form

$$\sigma_{ij}(t) = C_{ijkl}\sum_{m=1}^{M}\Delta_m\varepsilon_{kl} + \sum_{m=1}^{M} {}^{*}C_{ijkl}(t-t_m)\Delta_m\varepsilon_{kl} \tag{8}$$

Assuming that strains are smooth functions of time, and taking the limit as $\Delta_m t = t_{m+1} - t_m \to 0$ for all m, gives rise to

$$\sigma_{ij}(t) = C_{ijkl}\varepsilon_{kl}(t) + \int_{\tau=-\infty}^{t} {}^{*}C_{ijkl}(t-\tau)\frac{d\varepsilon_{kl}(\tau)}{d\tau}d\tau \tag{9}$$

where it is noted once again that the viscous moduli, ${}^{*}C_{ijkl}(t-\tau)$, are monotonically decreasing in time. Eq(9) is often referred to as the history integral for a linear Maxwell solid.

In many practical applications, adequate time-dependent stress predictions can be obtained with only several terms in the Prony series, Eq(4). The constitutive model as presented in Eq(9) requires that the history of the measurable kinematics, $\varepsilon_{kl}(\tau)$, be known in addition to the Prony series. This leads to computational algorithms that must determine how much of the history to retain in order to update the viscous stress approximation as time evolves.

MAXWELL SOLID IN DIFFERENTIAL FORM

Following Johnson et al.,[8-10] new constitutive equations for a linear viscous solid are derived. The new constitutive equations are in differential form and they are equivalent to the history integral form just described. Departing from the history integral formulation at Eq(6), defining internal strain variables, ${}^{*}_{n}\varepsilon_{kl}$, which relate to the strains as,

$$\Delta_m {}^{*}_{n}\varepsilon_{kl}(t-t_m) = H(t-t_m)e^{-\frac{(t-t_m)}{\tau_n}}\Delta_m\varepsilon_{kl} \tag{10}$$

introducing Eq(10) into Eq(6) and factoring out C^{*}_{ijkl}, the stresses appear as

$$\sigma_{ij}(t) = C_{ijkl}\sum_{m=1}^{M}\Delta_m\varepsilon_{kl} + C^{*}_{ijkl}\sum_{n=1}^{N}\sum_{m=1}^{M}\Delta_m {}^{*}_{n}\varepsilon_{kl}(t-t_m) \tag{11}$$

Following the Maxwell solid formulation, it is assumed that the strains are smooth functions of time. In the limit as $\Delta_m t = t_{m+1} - t_m \to 0$ for all m, Eq(11) becomes

$$\sigma_{ij}(t) = C_{ijkl}\varepsilon_{kl}(t) + C^{*}_{ijkl}\sum_{n=1}^{N}\int_{\tau=-\infty}^{t} d{}^{*}_{n}\varepsilon_{kl}(t-\tau) \tag{12}$$

It is desirable to derive a differential equation for the time dependent strain variables. In the limit as $\Delta_m t \to 0$, Eq(10) becomes

$$d{}^{*}_{n}\varepsilon_{kl}(t-\tau) = H(t-\tau)e^{-\frac{(t-\tau)}{\tau_n}}d\varepsilon_{kl}(\tau) \tag{13}$$

Integrating Eq(13) with respect to the history, τ, yields

$$ {}^{*}_{n}\varepsilon_{kl}(t) = \int_{\tau=-\infty}^{t} \frac{d\varepsilon_{kl}(\tau)}{d\tau} e^{-\frac{(t-\tau)}{\tau_n}} d\tau \tag{14} $$

Differentiating Eq(14) with respect to the current time, t, yields

$$ \frac{d\,{}^{*}_{n}\varepsilon_{kl}(t)}{dt} = -\frac{1}{\tau_n}\left[\int_{\tau=-\infty}^{t} \frac{d\varepsilon_{kl}(\tau)}{d\tau} e^{-\frac{(t-\tau)}{\tau_n}} d\tau \right] + \frac{d\varepsilon_{kl}(t)}{dt} \tag{15} $$

Substituting Eq(14) into Eq(15) yields the differential equations for the internal strain variables in the form

$$ \frac{d\,{}^{*}_{n}\varepsilon_{kl}}{dt} + \frac{{}^{*}_{n}\varepsilon_{kl}}{\tau_n} = \frac{d\varepsilon_{kl}}{dt} \qquad \text{for each } n. \tag{16} $$

Introducing Eq(14) into Eq(12) results in the stress equation given by

$$ \sigma_{ij}(t) = C_{ijkl}\varepsilon_{kl}(t) + C^{*}_{ijkl} \sum_{n=1}^{N} {}^{*}_{n}\varepsilon_{kl}(t) \tag{17} $$

Eqs(16) and (17) represent the constitutive model in differential form. Note that this particular form is for the case of a material with a relaxation modulus given by Eq(4). Also, for a material whose modulus is expressed by Eq(4), the constitutive model of Eqs(16) and (17) is equivalent to the history integral model given by Eq(9). In what follows, the differential form of the constitutive model is explored in the context of a higher-order beam theory and its associated finite element.

VISCOELASTIC HIGHER-ORDER BEAM

In this section a quasi-static Maxwell solid version of Tessler's[11] higher-order beam theory is formulated and a simple beam finite element is derived. The beam dimensions and sign convention are shown in Figure 1. The viscoelastic constitutive model for the beam that is consistent with Eqs(16) and (17) can be written in matrix form as

$$ \mathbf{s}(t) = \mathbf{C}\mathbf{e} + {}^{*}\mathbf{C} \sum_{n=1}^{N} {}^{*}_{n}\mathbf{e}(t) \tag{18} $$

and

$$ \frac{d\,{}^{*}_{n}\mathbf{e}}{dt} + \frac{{}^{*}_{n}\mathbf{e}}{\tau_n} = \frac{d\mathbf{e}}{dt} \qquad \text{for each } n. \tag{19} $$

where

$$\mathbf{s}^T = \left(\sigma_{xx},\ \sigma_{zz},\ \tau_{xz}\right)$$

$$\mathbf{e}^T = \left(\varepsilon_{xx},\ \varepsilon_{zz},\ \gamma_{xz}\right)$$

$$\overset{*}{n}\mathbf{e}^T = \left(\overset{*}{n}\varepsilon_{xx},\ \overset{*}{n}\varepsilon_{zz},\ \overset{*}{n}\gamma_{xz}\right)$$

$$\mathbf{C} = \begin{bmatrix} C_{11} & C_{13} & 0 \\ C_{13} & C_{33} & 0 \\ 0 & 0 & C_{55} \end{bmatrix} \text{ and } {}^{*}\mathbf{C} = \begin{bmatrix} {}^{*}C_{11} & {}^{*}C_{13} & 0 \\ {}^{*}C_{13} & {}^{*}C_{33} & 0 \\ 0 & 0 & {}^{*}C_{55} \end{bmatrix}$$

In this higher-order theory, the components of the displacement vector are approximated through the beam thickness by way of five kinematic variables, i.e.,

$$u_x(x,z,t) = u(x,t) + h\zeta\theta(x,t) \tag{20}$$

$$u_z(x,z,t) = w(x,t) + \zeta w_1(x,t) + \left(\zeta^2 - \frac{1}{5}\right)w_2(x,t) \tag{21}$$

where $\zeta = z/h$ denotes a nondimensional thickness coordinate and $2h$ is the total thickness. Note that $u(x,t)$ represents the midplane (i.e. reference plane) axial displacement, $\theta(x,t)$ is the bending rotation of the cross-section of the beam, $w(x,t)$ is the weighted-average deflection,[11] and $w_1(x,t)$ and $w_2(x,t)$ are the higher-order transverse displacement variables enabling a parabolic distribution of $u_z(x,z,t)$ through the thickness. The above displacement assumptions give rise to the following thickness distributions for the strains: a linear axial strain, a cubic transverse normal strain, and a quadratic transverse shear strain. [11] These strain components have the following form

$$\varepsilon_{xx} = u(x,t)_{,x} + h\zeta\theta(x,t)_{,x} \tag{22}$$

$$\varepsilon_{zz} = \frac{w_1(x,t)}{h} + \phi_z(\zeta)\frac{w_2(x,t)}{h^2} + \phi_x(\zeta)\,\theta(x,t)_{,x} \tag{23}$$

$$\gamma_{xz} = \phi_{xz}(\zeta)\left(w(x,t)_{,x} + \theta(x,t)\right) \tag{24}$$

where

$$\phi_x(\zeta) = \frac{h\nu_{13}\zeta\left(4 - 7\zeta^2\right)}{17},\quad \phi_z(\zeta) = \frac{14\zeta h\left(3 - \zeta^2\right)}{17},\quad \phi_{xz}(\zeta) = \frac{5\left(1 - \zeta^2\right)}{4}$$

The simplest finite element approximation of this beam theory, as explored in Ref. [11], involves a three-node configuration (see Figure 2) which is achieved by the following interpolations

$$u(\eta,t) = (1-\eta)u_0(t) + \eta u_1(t) \tag{25}$$

$$\theta(\eta,t) = (1-\eta)\theta_0(t) + \eta\theta_1(t) \tag{26}$$

$$w(\eta,t) = (1-\eta)w_0(t) + \eta w_1(t) - \frac{l}{2}\eta(1-\eta)\big(\theta_0(t) - \theta_1(t)\big) \tag{27}$$

$$w_1(\eta,t) = W_1(t) \tag{28}$$

$$w_2(\eta,t) = W_2(t) \tag{29}$$

where $\eta = x/l$ is the nondimensional element length coordinate. Note that the nodal degrees-of-freedom at the two ends of the element are subscripted with indices 0 and 1. Since the strains do not possess derivatives of the $w_1(\eta,t)$ and $w_2(\eta,t)$ variables, these variables need not be continuous at the element nodes and, hence, their simplest approximation is constant for each element. Their corresponding degrees-of-freedom are attributed to a node at the element midspan.

For a quasi-static loading, the virtual work statement for an element of volume V with the differential form of the Maxwell constitutive law included can be written as

$$\int \mathbf{e}^T \mathbf{C}\delta\mathbf{e}dV + \sum_{n=1}^{N}\int {}^*_n\mathbf{e}^T \mathbf{C}\delta {}^*_n\mathbf{e}dV - \delta W = 0 \tag{30}$$

where the first integral represents the internal virtual work done by the elastic stresses, the second is the internal virtual work done by the viscous stresses, and δW is the virtual work done by the external forces. Introducing Eqs(25)-(29) into Eqs(20)-(21) and substituting the results into Eqs(22)-(24) yields finite element approximations of the strains in terms of the nodal variables, i.e.,

$$\mathbf{e} = \mathbf{B}\mathbf{u} \tag{31}$$

where

$$\mathbf{B} = \begin{bmatrix} -\frac{1}{l} & 0 & -\frac{z}{l} & 0 & 0 & \frac{1}{l} & 0 & \frac{z}{l} \\ 0 & 0 & -\frac{\phi_x}{l} & \frac{1}{h} & \frac{\phi_z}{h^2} & 0 & 0 & \frac{\phi_x}{l} \\ 0 & -\frac{\phi_{xz}}{l} & \frac{\phi_{xz}}{2} & 0 & 0 & 0 & \frac{\phi_{xz}}{l} & \frac{\phi_{xz}}{2} \end{bmatrix} \tag{32}$$

and $\mathbf{u}^T = \left(u_0, w_0, \theta_0, W_1, W_2, u_1, w_1, \theta_1\right)$ denotes the element nodal displacement vector.

A set of analogous nodal variables, ${}^*_n\mathbf{u}$, and corresponding viscous strains, ${}^*_n\mathbf{e}$, are introduced. These are related by

$$ {}^{*}_{n}\mathbf{e} = \mathbf{B}\ {}^{*}_{n}\mathbf{u} \tag{33} $$

The virtual work statement for an element then becomes

$$ \mathbf{u}^{T}\int \mathbf{B}^{T}\mathbf{C}\mathbf{B}dV\delta\mathbf{u} + \sum_{n=1}^{N} {}^{*}_{n}\mathbf{u}^{T}\int \mathbf{B}^{T\,*}\mathbf{C}\mathbf{B}dV\delta\,{}^{*}_{n}\mathbf{u} - \delta W\ = 0 \tag{34} $$

By defining the integrals in Eq(34) as stiffness matrices , there results

$$ \mathbf{u}^{T}\mathbf{k}\ \ \delta\mathbf{u} + \sum_{n=1}^{N} {}^{*}_{n}\mathbf{u}^{T\,*}\mathbf{k}\ \ \delta\,{}^{*}_{n}\mathbf{u} - \delta W\ = 0 \tag{35} $$

Since Eq(19) implies $\delta\mathbf{e} = \delta\,{}^{*}_{n}\mathbf{e}$ when t is constant, the virtual work takes on a simpler form

$$ \left[\ \mathbf{u}^{T}\mathbf{k}\ \ + \sum_{n=1}^{N} {}^{*}_{n}\mathbf{u}^{T\,*}\mathbf{k}\ \right]\delta\mathbf{u} - \delta W\ = 0 \tag{36} $$

This implies that at any given time the element equilibrium equations are

$$ \mathbf{k}\ \mathbf{u} + \sum_{n=1}^{N} {}^{*}\mathbf{k}\ {}^{*}_{n}\mathbf{u} = \mathbf{f} \qquad \text{for each element} \tag{37} $$

where $\mathbf{f}$ denotes the element consistent load vector due to the external loading. Introducing Eqs(31) and (33) into the differential equations for the strain variables in Eq(19) yields

$$ \frac{d\,{}^{*}_{n}\mathbf{u}}{dt} + \frac{{}^{*}_{n}\mathbf{u}}{\tau_{n}} = \frac{d\mathbf{u}}{dt} \qquad \text{for each } n \tag{38} $$

The global equilibrium equations are determined by the standard assembly of the element equations, Eqs(37). Note, there is no assembly for Eqs(38). The variables ${}^{*}_{n}\mathbf{u}$ are independent from element to element (recall, these variables carry the time dependent information for the material within the element). The global equilibrium equations at a given time are

$$ \mathbf{K}\mathbf{u}_{g} = \mathbf{F}_{mech} - \mathbf{F}_{visc} \tag{39} $$

where $\mathbf{u}_{g}$ denotes the global nodal variable vector, $\mathbf{K}$ is the elastic stiffness matrix, $\mathbf{F}_{mech}$ is the global force vector due to mechanical loads, and $\mathbf{F}_{visc}$ is the assembled vector for $\sum_{n=1}^{N} {}^{*}\mathbf{k}\ {}^{*}_{n}\mathbf{u}$. The viscoelastic problem is solved by simultaneously integrating

the differential and algebraic equations expressed by Eqs(38) and (39), where the latter is subject to the appropriate boundary restraints.

As far as the finite element implementation is concerned, a conventional linearly elastic code can be readily adapted to perform the viscoelastic analysis for a Maxwell material, i.e., for a material whose relaxation stiffness coefficients can be modeled with a Prony series. First, the instantaneous stiffness coefficients, ${}^{*}C_{ijkl}$, are used in place of the elastic values to compute the element viscous stiffness matrices, ${}^{*}\mathbf{k}$, which are stored for repeated use. The internal nodal variables for each element, ${}^{*}_{n}\mathbf{u}$, are set equal to their initial values and stored. A predictor-corrector algorithm is then used to integrate Eqs(38) and (39) in time. The predictor-corrector integration algorithm used in this effort is described in the Appendix.

APPLICATIONS

Numerical solutions representative of stress relaxation, creep, and cyclic creep for a thick orthotropic beam are presented. The beam elastic stiffness coefficients ($\mathbf{C}$ matrix in Eq (18)) for the state of plane stress can be written in terms of engineering material constants as

$$C_{11} = \frac{E_x}{1-\nu_{xz}\nu_{zx}}\ , \quad C_{33} = \frac{E_z}{1-\nu_{xz}\nu_{zx}}, \quad C_{13} = \nu_{xz}C_{33}, \quad C_{55} = G_{xz}$$

A unidirectional E-glass/epoxy laminate is considered for which the material constants are: $E_x = 38.6\ GPa$, $E_z = 8.27\ GPa$, $G_{xz} = 4.14\ GPa$, $\nu_{xz} = 0.26$, and $\nu_{zx} = \nu_{xz}E_x/E_z$. The viscous relaxation properties were computed from complex modulus vs. frequency data for the E-glass/epoxy reported in Ref[12]. The equations for the real and imaginary parts of the modulus of a Maxwell series were least-squares fit to the data in a frequency range of 45 Hz – 145 Hz. The least squares fit was performed with the constraint that the moduli in the Maxwell series each be positive. The series was defined with ten time constants; τ_n= 1.0E-4, 3.162E-4, 1.0E-3, 3.162E-3, 1.0E-2, ... , 1.0E+1, and infinity. The Prony series was scaled so that its equivalent static value (at t equal to infinity) was unity. The resulting series is

$$P(t) = 1.0 + 0.01755\ e^{-0.0001t} + 0.000257\ e^{-0.01t} + 0.072014\ e^{-0.3162t}$$

The time dependent stiffness values for the E-glass/epoxy are given by $\mathbf{C}^{v} = \mathbf{C}P(t)$. The beam dimensions are as follows: $L = 0.1m$, $2h = 0.02m$, and $b = 0.01m$ (refer to Figure 1).

Example 1. A cantilever beam with w, u, θ fixed at point A has a prescribed deflection w at point B that is ramped from 0 to -1 cm in 0.05 sec and then held constant at -1 cm. Figure 3 depicts the value of the maximum axial stress computed at point D as a function of time. Also shown are the elastic and viscous stress components comprising the total stress. The decay of the total viscoelastic stress to its elastic value as time is increased demonstrates the expected step-strain relaxation behavior.

Example 2. A simply-supported beam with w and u fixed at point A and w fixed at point B is subject to a uniform, top-surface pressure, $q^+(t)$. The time-dependent value of the pressure is ramped from 0.0 to 1.0 MPa in 0.05 sec and then held constant. Figure 4 shows the value of the w deflection at the midspan of the beam. The viscous solution shows the expected creep response.

Example 3. The simply-supported beam in the preceding example is subject to a harmonic pressure loading given by

$$q^+(t) = 0, \quad t \le 0 \text{ and } q^+(t) = 0.05 * \left(1 - \cos(50\pi t)\right) \; MPa, \quad t > 0$$

Figure 5 depicts the transverse normal stress and strain values at the midspan (point C) versus time. The upward drift of the maximum and minimum values of the strain demonstrates cyclic creep.

CONCLUSION

A differential form of the Maxwell viscous solid constitutive theory has been derived and implemented within a higher-order-theory beam finite element. The finite element formulation is attractive for several reasons: (1) The constitutive constants are the same as those needed in the classical history-integral model, and they are also readily available from step-strain relaxation tests, (2) The state variables are conjugate to the elastic strain measures; hence, they are consistent with the kinematic assumptions of the elastic formulation, (3) The update of the state variables can be performed in a parallel computing environment, allowing the viscous force vector in the equations of motion to be determined efficiently within the predictor-corrector algorithm, (4) Applications of time-dependent displacements and loads are performed within the same finite element algorithm, and (5) The higher-order beam theory accounts for both transverse shear and transverse normal

deformations — the effects that need to be accounted for in thick and highly orthotropic beams and high-frequency dynamics.

The computational examples for the problems of relaxation, creep, and cyclic creep clearly demonstrated the predictive capabilities of the finite element formulation.

REFERENCES

1. Halpin, J. C., and Pagano, N. J., Observations on linear anisotropic viscoelasticity, J. Composite Materials, **2**, No. 1, 68-80 (1968).

2. Hashin, Z., Complex moduli of viscoelastic composites - I. General theory and applications to particulate composites, Int. J. Solids Structures, **6**, 539-552 (1970).

3. Hashin, Z., Complex moduli of viscoelastic composites - II. Fiber reinforced materials, Int. J. Solids and Structures, **6**, 797-807 (1970).

4. Argyris, J., St. Doltsinis, I., and daSilva, V. D., Constitutive modelling and computation of non-linear viscoelastic solids, Part I. Rheological models and numerical integration techniques, Comput. Methods Appl. Mech. Engrg., **88**, 135-163 (1991).

5. Shaw, S., Warby, M. K., and Whiteman, J. R., Numerical techniques for problems of quasistatic and dynamic viscoelasticity, in "The Mathematics of Finite Elements and Applications," edited by J. R. Whiteman, John Wiley & Sons (1994).

6. Coleman, B. D., and Noll, W., Foundations of linear viscoelasticity, Reviews of Modern Physics, **33**, No.2, 239-249 (1961).

7. Schapery, R. A., Viscoelastic behavior and analysis of composite materials, in "Composite Materials", **2**, edited by G. P. Sendeckyj, Academic Press (1974).

8. Johnson, A. R., and Stacer, R. G., Rubber viscoelasticity using the physically constrained system's stretches as internal variables, Rubber Chemistry and Technology, **66**, No.4, 567-577 (1993).

9. Johnson, A. R., Tanner, J. A., and Mason, A. J., A kinematically driven anisotropic viscoelastic constitutive model applied to tires, in "Computational Modeling of Tires," compiled by A. K. Noor and J. A. Tanner, NASA Conference Publication 3306, August 1995.

10. Johnson, A. R., Tanner, J. A., and Mason, J. A., A viscoelastic model for tires analyzed with nonlinear shell elements, presented at the Fourteenth Annual Meeting and Conference on Tire Science and Technology, University of Akron, March 1995.

11. Tessler, A., A two-node beam element including transverse shear and transverse normal deformations, Int. J. for Numer. Methods Eng., **32**, 1027-1039 (1991).

12. Gibson, R. F., and Plunkett, R., Dynamic mechanical behavior of fiber-reinforced composites: Measurement and analysis, J. Composite Materials, **10**, 325-341 (1976).

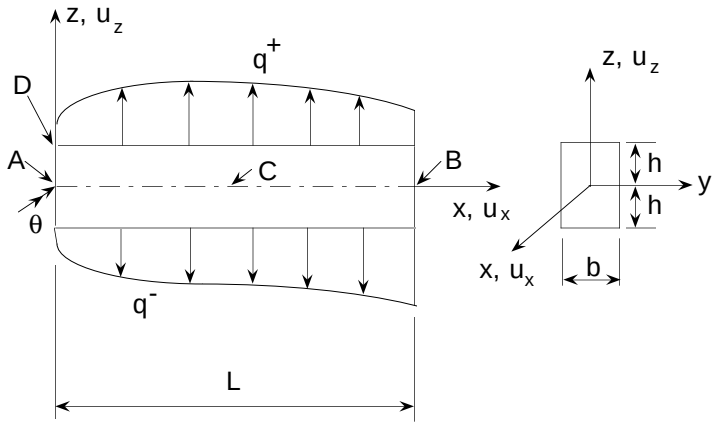

Boundary conditions applied at points A & B.

Stresses and displacements computed at C & D.

Figure 1. Thick-beam geometry, kinematics, and loading.

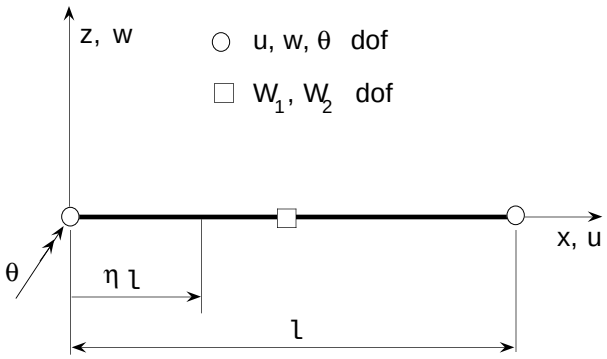

Figure 2. A three-node, higher-order-theory thick-beam element.

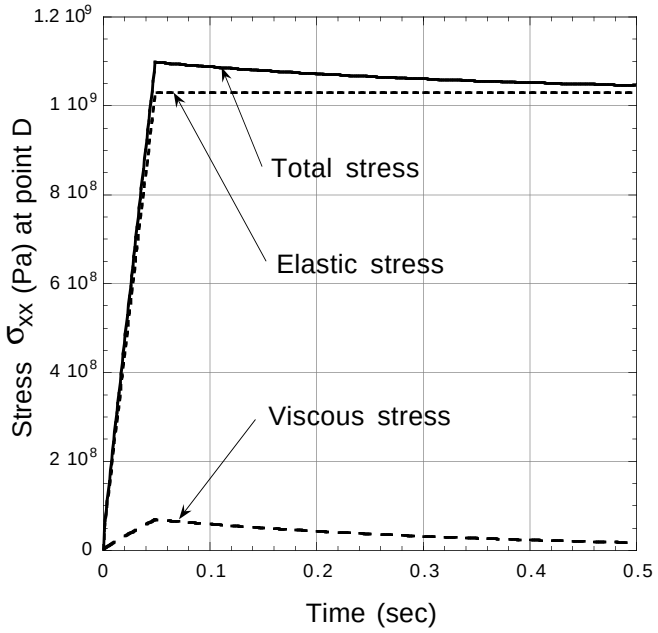

Figure 3. Cantilevered beam under prescribed tip deflection. Stress in top surface at support.

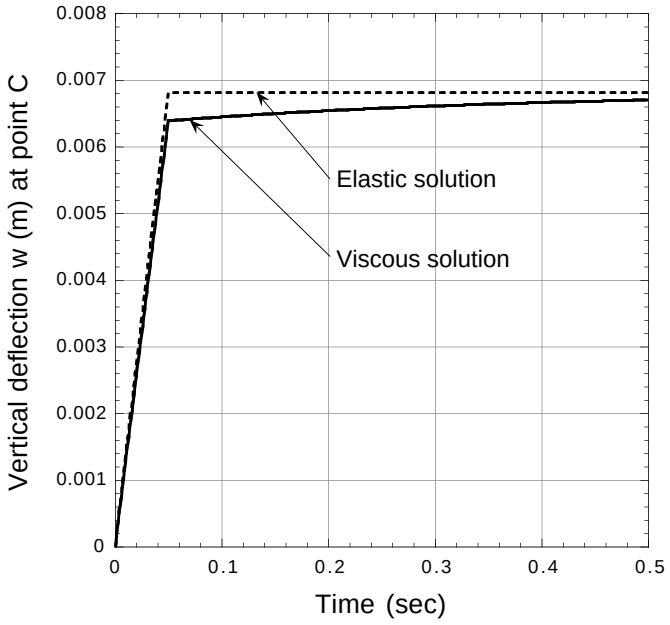

Figure 4. Simply-supported beam under prescribed pressure loading. Weighted-average deflection,w, at center of beam.

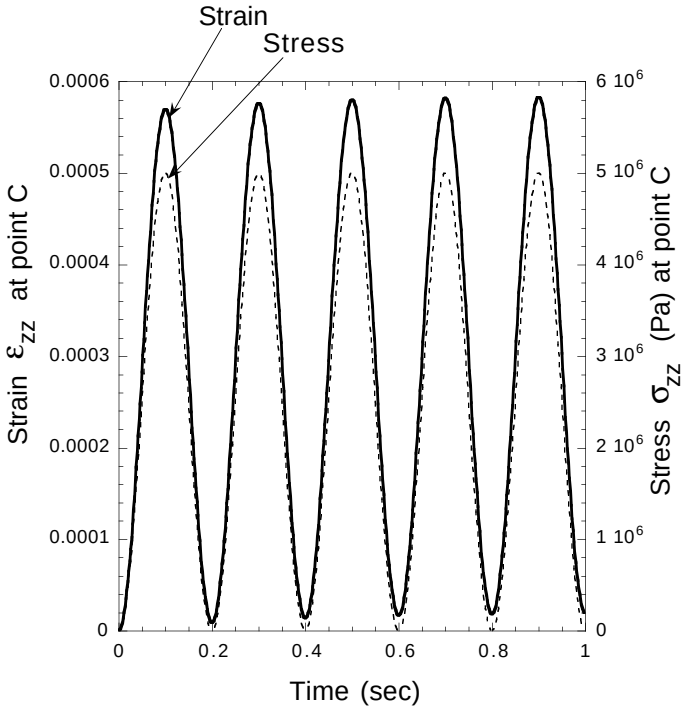

Figure 5. Simply-supported beam under harmonic pressure loading. Transverse normal strain and stress at beam center versus time.

APPENDIX

The predictor-corrector integration algorithm is described below. The storage requirements, beyond the requirements for the elastic problem, involves two sets of vectors, ${}^{*}_{n}\mathbf{u}$, for each element, two global vectors, $\mathbf{u}_g$, a global force vector, $\mathbf{F}_{visc}$, a full set of element viscous stiffness matrices, ${}^{*}\mathbf{k}$, and a matrix which carries the Prony series information for each element. The time integration algorithm used in this effort provides a trapezoidal solution to the differential equations while simultaneously solving the algebraic equilibrium equations. The elastic (static) finite element code already contains the assembly and solver subroutines needed. Building the viscous (quasi-static) finite element code only requires that additional storage be allotted and a few modified call statements be added. The algorithm is outlined below.

Time Integration Algorithm

A. Initialize variables ($1 \Rightarrow t$, $2 \Rightarrow t + \Delta t$)

$${}^{*}_{n}\mathbf{u}_2 = \mathbf{0} \quad \forall \text{ elements.}$$

$$\mathbf{u}_{g,2} = \mathbf{0}$$

$$\beta_{1n} = \left(\frac{1 - \dfrac{\Delta t}{2\tau_n}}{1 + \dfrac{\Delta t}{2\tau_n}} \right) \text{ integration constant.}$$

$$\beta_{2n} = \left(\frac{1}{1 + \dfrac{\Delta t}{2\tau_n}} \right) \text{ integration constant.}$$

B. Move data to next time step.

$${}^{*}_{n}\mathbf{u}_1 = {}^{*}_{n}\mathbf{u}_2 \quad \forall \text{ elements.}$$

$$\mathbf{F}_{mech,1} = \mathbf{F}_{mech,2}$$

$$\mathbf{F}_{visc,1} = \mathbf{F}_{visc,2}$$

$$\mathbf{u}_{g,1} = \mathbf{u}_{g,2}$$

$$t = t + \Delta t$$

$$\mathbf{F}_{mech,2} = \mathbf{F}_{mech}(t)$$

$$\mathbf{u}_{g,2} = \mathbf{K}^{-1}\left[\mathbf{F}_{mech,2} - \mathbf{F}_{visc,1}\right] \text{ seed for Step C.}$$

C. Update internal variables (element components of global vectors implied).

$${}^{*}_{n}\mathbf{u}_2 = \beta_{1n}\,{}^{*}_{n}\mathbf{u}_1 + \beta_{2n}\left(\mathbf{u}_{g,2} - \mathbf{u}_{g,1}\right)$$

D. Update viscous forces.

$$\mathbf{F}_{visc,2} \quad \text{assemble} \sum_{n=1}^{N} {}^{*}\mathbf{k}_n\,{}^{*}_{n}\mathbf{u}_2$$

E. Update global displacements.

$$\mathbf{u}_{g,2} = \mathbf{K}^{-1}\left[\mathbf{F}_{mech,2} - \mathbf{F}_{visc,2}\right]$$

F. If changes to $\mathbf{u}_{g,2}$ are small then go to Step B.

Else go to Step C.